역암의 역학적 거동 특성 파악을 위한 개별요소법의 응용
DEM estimation of mechanical properties of conglomeratic rocks

박영도[1], Youngdo Park, 유승학[2], Seung-Hak Yoo·, 김기석[3], Ki-Seok.Kim

[1] (주) 희송지오텍 상무이사, Director, Research Division, Heesong Geotek Co., Ltd.
[2] (주) 희송지오텍 과장, Manager, Heesong Geotek Co., Ltd.
[3] (주) 희송지오텍 대표이사, President, Research Division, Heesong Geotek Co., Ltd.

개요 : 역들의 공간적 분포가 불균질하고 역의 크기가 큰 역암의 경우 암석 전체를 대표하는 물성치 (E_m, c, ϕ 등)를 구하기 위해서는 매우 큰 시험기기가 필요하다. 따라서, 커다란 역을 포함하는 역암의 경우, 직접 암석실내시험을 통한 물성치 산정은 현실적으로 거의 불가능하다. 이러한 문제를 극복하기 위하여 이 연구에서는 개별요소법을 이용하여 역암의 물성치를 산출하는 방법을 제안한다. 그 방법은 다음과 같다. (1) 역암내의 역의 물성과 기질부의 물성을 각각 실내실험을 통하여 파악한 후 (2) 이들 두 물질의 거동양상을 구현할 수 있는 개별요소집합체의 개별요소간의 물성을 결정한다. (3) 역의 함량, 크기, 모양, 공간적 분포양상등의 역암 조직과 유사한 개별요소 수치해석시료를 만든 후, (4) 이를 수치해석실험 (이축압축실험) 에 사용한다. 이러한 수치해석실험을 통해 현재까지 만들어진 결과는 다음과 같다. 첫째, 역의 강도가 기질의 강도보다 높은 역암의 경우, 역의 양이 증가할수록 일축압축강도, 내부마찰각, 점착력이 증가하지만 증가 양상은 선형이 아니다. 탄성계수의 경우 역의 양과 상관 없이 변화하지 않는다. 둘째, 역과 기질 사이 표면의 점착력이 약할 경우 이러한 표면에서 최초 미세 균열이 형성되기 시작하므로 이 점착력은 물성치를 산출하는 중요한 인자이다. 따라서, 향후 이에 대한 자세한 연구가 필요하다고 판단된다. 결론적으로, 설계 또는 시공시 직접시험에 의한 물성치의 파악이 어려운 역암 또는 직접시험을 위해 대량의 시료를 필요로 하는 함력 미고결지층, 핵석층, 풍화암과 같은 시료의 물성치는 별도로 측정된 물성들 (예, 역과 기질)을 이용한 개별요소법을 통해 구할 수 있다.

주요어 : 개별요소법, 역암의 물성치 산정, 수치해석, 핵석층, 풍화암

1. Introduction

Elastic properties of rocks have fundamental importance in geotechnical engineering because they are used in designing to estimate and determine the type and amount of reinforcement. For this reason, most of construction standards require that elastic properties of rocks in construction sites should be measured. The measurement of elastic properties of rocks is usually carried out using standard testing equipment (e.g. uniaxial and triaxial tests, Brazilian test). However, when the sample size should be large to ensure representative properties, it becomes difficult to use the standard testing equipment because of size limitations. One of the representative examples of such case is conglomeratic rocks containing finer matrix and larger sedimentary clasts with usually higher strength. Conglomeratic rocks usually form in depositional environments where the current has high energies (e.g. fan delta). In South Korea, most of conglomeratic rocks are found at the base of the Kyungsang Supergroup in the Kyungsang basin and in smaller Cretaceous basins formed at releasing bands of strike-slip

faults (e.g. Jinan basin). For mechanical test of conglomeratic rocks containing clasts larger than boulders (64~256 mm) in relatively weaker and fine-grained matrix, a very large equipment would be necessary for direct measurement of elastic properties. Thus, it is nearly impossible to obtain elastic properties for these rocks by direct measurement.

In this paper, we propose a numerical test using a DEM code (distinct element method) to overcome size-related problems described above. We used PFC 2D (developed by Itasca Consultant Group; PFC hereafter) to estimate the elastic properties of conglomeratic rocks by preparing a numerical specimen containing matrix and larger sedimentary clasts (LSCs hereafter). PFC has been used to solve the similar type of problems for jointed rocks (e.g. Cundall, 2000; Park et al, 2004). One fundamental difference between DEM-based PFC and continuum codes (e.g. FEM) is that there are micromechanical properties and constitutive equations that govern the motion of *each* distinct element in DEM-based PFC, whereas the governing constitutive equations and input values of mechanical properties determine the *system* behavior in continuum codes. Thus, for modeling with PFC, it is necessary to find out, by trial and errors, the micromechanical properties that will eventually determine the macroscopic behavior of the material that one intends to model. PFC has been used in wide disciplines of science and engineering (e.g. geology, rock mechanics and pharmaceuticals; Shimizu et al 2004; Park et al, 2004, Lee et al, 2004), since PFC is capable of showing pattern formation related to emergence. Emergence, here, refers to the system behavior with macroscopically complicated characteristics resulting from far simpler governing laws at micro scale (Hobbs, 2004).

In this study, it will be shown how DEM-based PFC can be applied to estimate the bulk elastic properties of conglomeratic rocks containing materials with contrasting mechanical properties. Some preliminary results along with some important controlling factors that affect the bulk elastic properties will also be discussed.

2. Description of Numerical experiments

The basic data structures of PFC are balls and walls. Balls are used to represent the material for mechanical modeling and walls are used to represent boundary conditions. Balls in PFC are considered as elastic, and elastic energy due to the overlap among balls is the driving force for deformation within the system. Balls can be grouped to represent the particles of various shapes. Grouping of balls can be done by applying 'clump logic', 'contact bond' or 'parallel bond' to the balls in contact. While clumped balls never break apart, balls with bonds can also be broken apart when the applied stress between balls exceeds the bond strength. Details of the bond logic can be found in the PFC manual (Itasca Consultant Group, 1995).

In this study, we used ball aggregates bonded with parallel bonds to make model rocks. Parallel bond was chosen because ball aggregates with parallel bond showed elastic properties similar to rocks. Most of the commands and FISH codes (built-in language in PFC) that we used in our numerical experiments were developed by Potyondy et al (1996). Some modifications are made to these codes in order to implement LSCs in the numerical specimen and to assign different properties to LSCs and LSC-to-matrix interfaces.

2.1 Numerical specimen

The ball aggregates consist of balls with varying sizes with the size range of 1 to 3 (min to max). The size distribution of balls between the size range is set to be uniform. This type of size distribution is chosen to avoid crystalline packing that will result in cracking at preferred orientations when balls with identical size are used. After generation of balls, the ball radii are increased by multiplying the user-defined factor until the number of contacts with the surrounding balls becomes at least three for every ball in the system.

Parallel bonds with different strengths are applied for three different types of interfaces (Figure 1); (1) matrix-to-matrix interface, (2) LSC-to-LSC interface, and (3) LSC-to-matrix interface. This was done by finding all of the balls in contact by searching the linked list with contact pointers. The contact type is determined using predefined flags assigned to balls. When two balls are in contact with each other, the diameter of the smaller balls is set to be the width of the cementing material for parallel bond (Figure 1). We assumed that matrix and LSC are made of sandstone and granite, respectively, for most of our numerical experiments (shown in Figures 2 to 4). Details of the micromechanical properties are listed in Table 1.

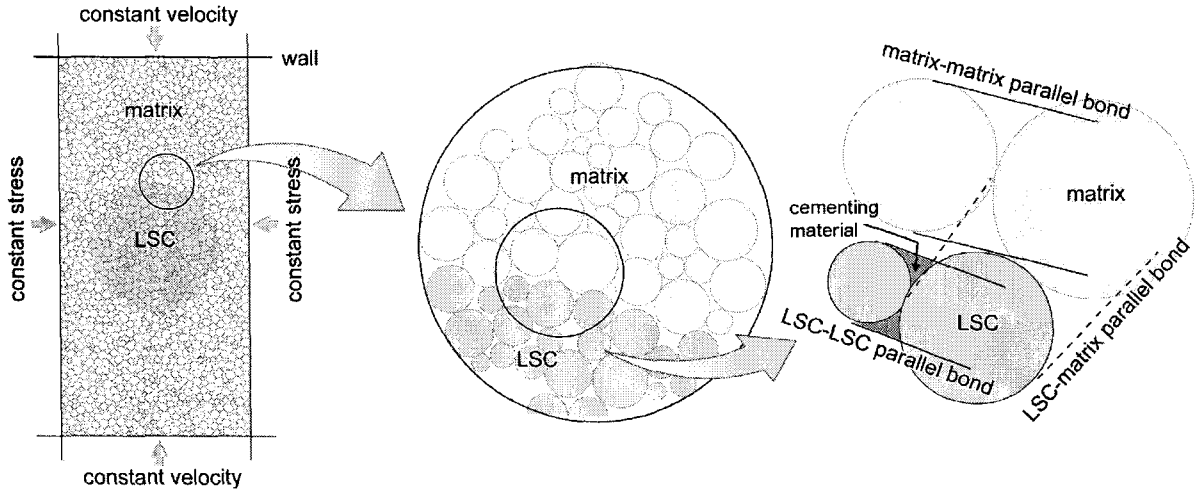

Figure 1. Numerical specimen and boundary condition.

Table 1. List of micromechanical properties for the representation of rocks using ball aggregates.

Rock type	sandstone (matrix)	granite (LSC)
range of ball size (m)	0.05~0.16	0.05~0.16
ball density (Kg/m^3)	2630	2630
ball friction	0.5	0.5
normal stiffness (GPa)	124	124
shear stiffness (GPa)	60	60
strength of paralle bond (MPa)	50	160
normal stiffness of cementing material for parallel bonds (GPa)	62/L*	62/L*
shear stiffness of cementing material for parallel bonds (GPa)	25/L*	25/L*

L*: sum of radii of two balls in contact

2.2 Boundary conditions for biaxial test

Two sets of wall are used for the representation of boundary conditions in the numerical experiments. Constant velocity is imposed on the horizontal walls in Figure 1. The horizontal walls approach to each other and serve as rigid platens providing the driving force for deformation. The vertical walls in Figure 1 are equipped with a numerical servo mechanism. The numerical servo mechanism on the vertical walls maintains constant normal stress by monitoring the normal stress exerted by ball aggregates and adjusting wall positions. Therefore, constant confining pressure can be maintained during mechanical test. The numerical codes written in FISH also record the wall positions as well as the normal stresses acting on two sets of the walls, allowing to construct the stress-strain curve. Confining pressures ranging from 0.1 MPa to 50 MPa (0.1, 2.5, 5, 10, 25, 50 MPa) were applied in order to estimate the internal friction angle and cohesion of the ball aggregates.

3. Results

Several sets of numerical experiments were carried out to see the effect of various controlling factors. First, numerical tests were made to determine the properties of the two single phases (matrix and LSCs) that constitute conglomeratic rocks (Figure 2; Table 2). Second, the amount of LSCs is varied to investigate the effect of the volume percentage of stronger LSCs on the elastic properties (Figures 3 and 4; Table 2). Third, we have investigated two possible case; one with weaker LSCs (Figure 5a; Table 2) and the other with weaker interfacial cohesion (strength of parallel bond) between matrix and LSCs (Figure 5b; Table 2).

For the determination of elastic properties of matrix and LSCs in conglomeratic rocks, experiments only with single matrix phase (sandstone) and single LSC phase (granite) were carried out. The experimental results are summarized in Table 2. Figure 2 shows development of cracks in matrix material. Most of earlier cracks (Figure 2a) are oriented subparallel to σ_1 direction, while the sites for crack initiation are somewhat evenly distributed. Stages from Figure 2b to 2c show crack propagation at tips of 'crack aggregates' (brittle shear zones formed by coalescence of individual cracks) which are oriented at 25~30° from σ_1 direction. When crack linkage by propagation reaches to a certain level, strength starts to drop marking the peak strength of the numerical specimen (Figure 2d). Figure 2e shows cumulative number of cracks during the test. The number of mode I cracks is far greater than the number of mode II cracks. It is also worth noting that the crack aggregates behave like mode II crack macroscopically but individual cracks have mode I crack origins.

Table 2. Conditions and results of numerical tests.

area % and number (n) of LSCs	uniaxial compressive strength (MPa)	elastic modulus (GPa)	poisson ratio	coheson (MPa)	angle of internal friciton (ϕ)	rock type
0 (N/A)	73.1	74.1	0.3	26.1	21.2	matrix*
100 (N/A)	213.6	74.4	0.3	67.2	27.5	granite+
10.7 (n=3)	73.0	74.1	0.3	26.0	21.4	conglomerate
16.8 (n=5)	73.3	74.0	0.3	26.7	20.9	conglomerate
23.7 (n=10)	78.7	74.9	0.3	28.1	21.0	conglomerate
31.0 (n=15)	79.7	75.0	0.3	28.1	21.5	conglomerate
34.1 (n=20)	83.2	75.0	0.3	28.3	22.9	conglomerate
36.5 (n=25)	86.5	74.1	0.3	28.7	24.7	conglomerate

*experiment to determine properties for matrix (sandstone)
+experiment to determine properties for LSC (granite)

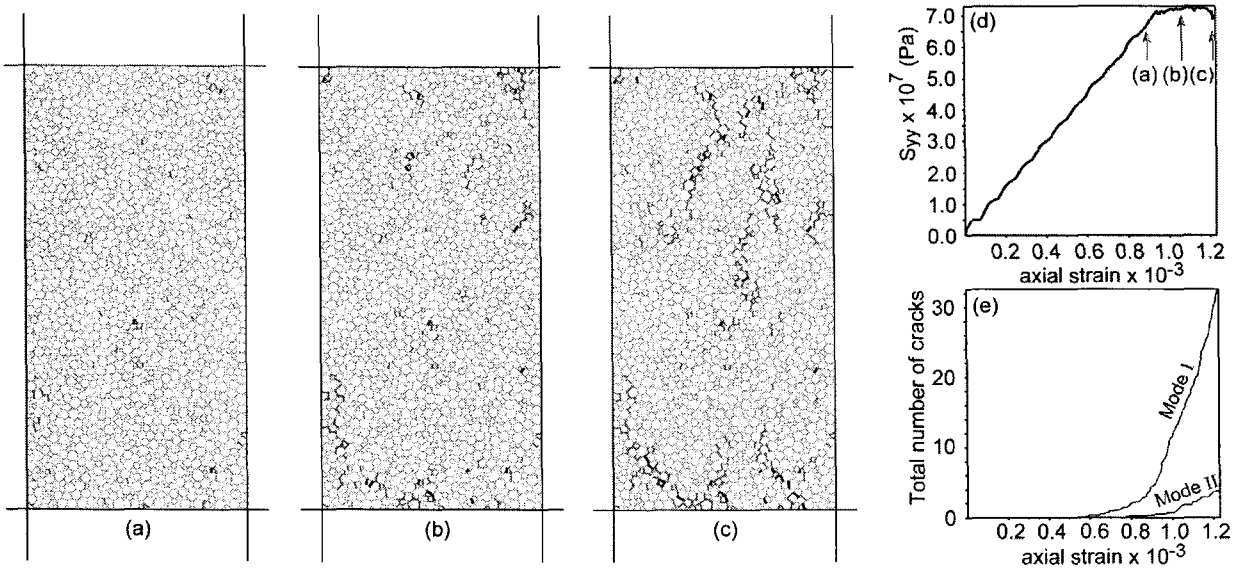

Figure 2. Crack initiation, propagation and linkage during biaxial test of specimen containing no LSCs (larger sedimentary clasts). (a) Crack initiation at step 5000, (b) crack growth at step 6000, (c) crack linkage at step 7000, (d) Stress-strain curve, (e) Evolution of total number of cracks (mode I and II) up to step 7000.

For the determination of elastic properties of mixtures of weaker matrix and stronger LSCs (described in Table 2), mechanical tests were performed for varying percentage (11~37 in area %) of LSCs (Figures 3 and 4). The strength (of parallel bond) for the LSC-to-matrix interfaces is assumed to have the value identical with that for the matrix-to-matrix interfaces (50 MPa). It is found that uniaxial compressive strength, internal friction angle and cohesion increase non-linearly with the percentage of LSCs while Young's modulus does not show such increase (Figure 4). The patterns of crack propagation (or formation of brittle shear zones) in Figure 3 can be divided into two groups depending on the volume percentage of LSCs. For

samples with lower volume percentage of stronger LSCs (Figure 3a, b, and c), the pattern of crack propagation and linkage is similar to that in LSC-free sample (Figure 2c). However, for samples with higher volume percentage of LSCs (Figure 3d, e and f), localization occurs along the connected weaker matrix.

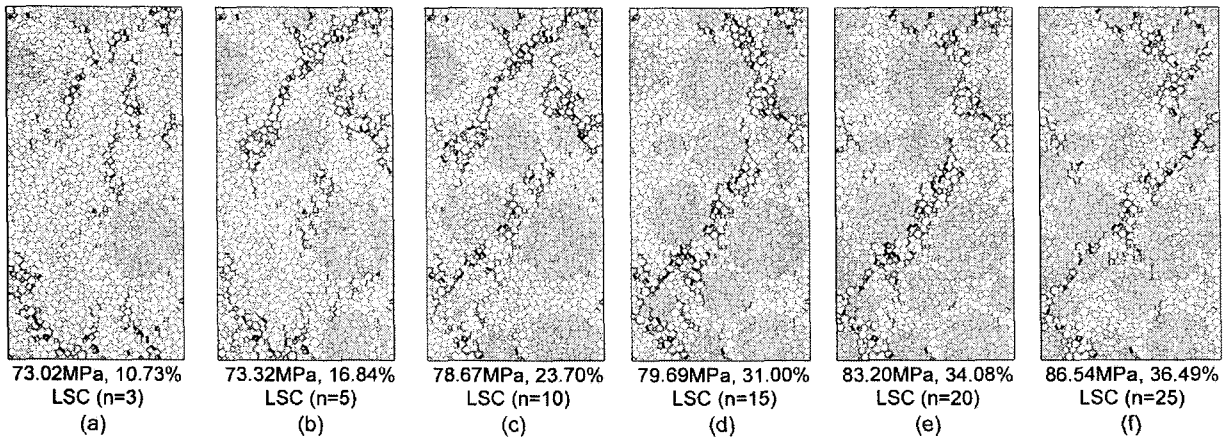

Figure 3. Development of brittle shear zones (failure planes) in sample with varying percentage of stronger LSCs (larger sedimentary clasts). Numbers with MPa units and % indicate uniaxial compressive strength and area percentage of larger sedimentary clasts, respectively.

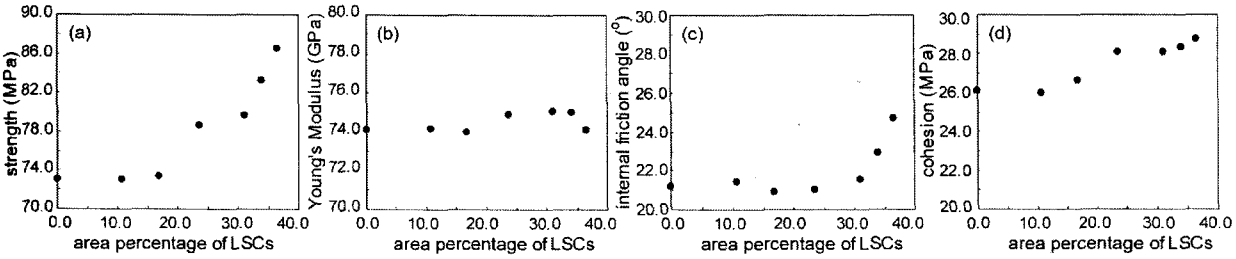

Figure 4. Plots of mechanical properties vs. amount of LSCs (larger sedimentary clasts). (a) uniaxial compressive strength, (b) Young's modulus, (c) internal friction angle, (d) cohesion.

Mechanical tests for conglomeratic rocks with weaker LSCs (10 MPa of parallel bond strength) and weaker interfacial cohesion (10 MPa of parallel bond strength) between matrix and LSC were also carried out. When a weaker LSC is present in the matrix, crack initiation starts in the LSC because of its weaker strength, and crack propagation toward the surrounding matrix occurs in the direction subparallel to σ_1 direction (Figure 5a). For samples with weaker interfacial cohesion, crack initiation starts at matrix-LSC interfaces oriented subparallel to σ_1 direction (Figure 5b), which is not surprising because of the presence of weaker cohesion around the LSC.

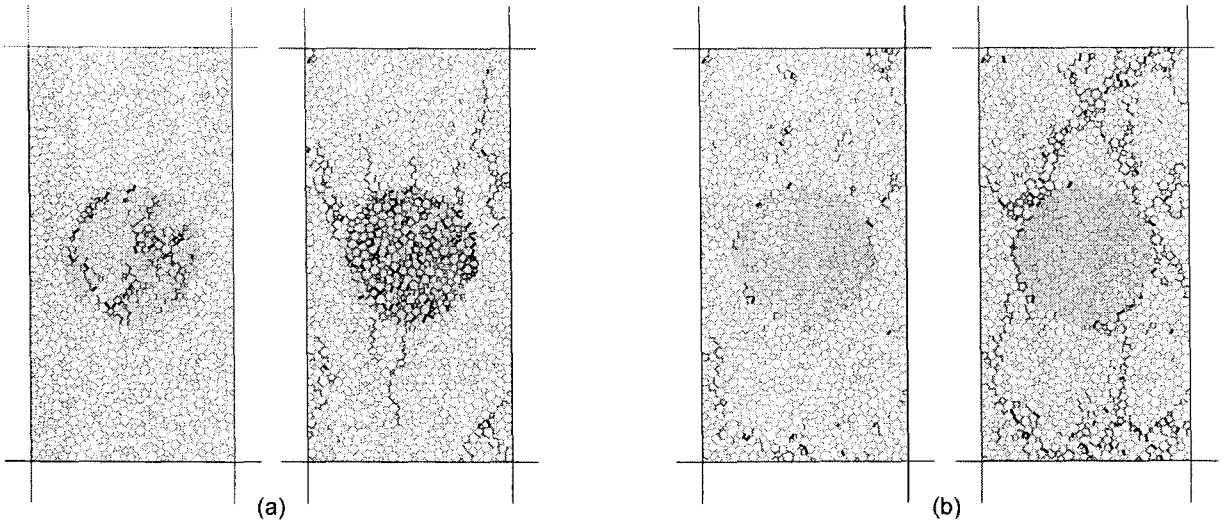

Figure 5. Development of brittle shear zones (failure planes) with a LSC (larger sedimentary clast) with weaker strength, and (b) with lower interfacial bond strength between matrix and larger sedimentary clasts.

4. Discussion

The results in Figure 4 demonstrate that the elastic properties are not linearly changing with the volume percentage of LSCs. Thus, for the estimation and use of the elastic properties of LSC-bearing conglomeratic rocks which are too large to do physical tests, we suggest to combine the results from both physical and numerical tests. For example, the elastic properties of LSCs can directly be measured with the core-size samples by the conventional small scale testing equipment. The properties of matrix can also be measured in a similar way. Then, numerical tests (discussed in this study) can be combined with the results from physical tests to produce the elastic properties of the whole rock.

So far, we have restricted our discussion to conglomeratic rocks, but extension of the results can be made to some other cases. For example, the results can be applied to the estimation of unlithified sediments with larger boulders and core-stone-bearing saprolite. Since the matrix in unlithified sediments and saprolite has weaker cohesion, ball aggregates with weaker bond or unbonded ball aggregates may be proper choices for the simulation of these material.

As demonstrated in Figure 3, the distribution geometry of LSCs is an important factor that controls the route for crack propagations. The geometry of larger sedimentary clasts, including size, size distribution, shape and spatial distribution, varies with depositional environments which may change over time. Since these geometric features have profound effect on determining mechanical properties and geometric features in conglomeratic rocks can change due to changes in depositional environment, we suggest detailed geometric analysis of conglomeratic rocks for numerical analysis.

The interfacial cohesion between LSC and matrix can also be an important factor because crack initiation can occur at interfaces if the interfacial strength is weaker. Despite the importance, it may be difficult to use the value measured directly from physical experiments. One possible way of rough estimation of the cohesion between LSC and matrix is to examine the sites for crack initiation from the physical samples after mechanical tests. Depending on

the relative values of cohesion among LSC-LSC, LSC-matrix and matrix-matrix interfaces, the initiation sites for cracks may be different. However, it would be still problematic when the LSC-matrix interface turns out to be the weakest among the three interfaces. In this case, one way of estimating interfacial cohesion will be to compare the results from physical experiments using smaller sedimentary-clast-bearing conglomerates with the results obtained by varying interfacial cohesion in numerical experiments. Once the interfacial cohesion is determined in this manner, the cohesion value can be applied to numerical modeling for LSC-bearing conglomerates. One final note about the interfacial cohesion is that interfacial cohesion is likely to be related to the surface roughness of LSCs because cementing between LSC and matrix is affected by roughness. Since the distance between sedimentary source and basin controls the roundness and roughness of LSCs, we suggest that detailed sedimentologic analysis for conglomeratic rocks should be carried out.

Finally, the numerical experiments described in this study were done using two dimensional code. Since the extension into three dimensions is trivial, we suggest three dimensional analysis for the better estimation of the elastic properties.

5. Conclusions

From the numerical experiments and analysis of the experimental results, we suggest the following.

(1) For conglomeratic rocks with larger sedimentary clasts that are too large to do physical tests, estimation of elastic properties can be made by the following two steps; (i) determination of individual elastic properties of clasts and matrix by physical tests and (ii) estimation of the properties by numerical experiments with the individual elastic properties determined by physical experiments.

(2) For conglomeratic rocks with stronger LSCs, it is found that the uniaxial compressive strength, internal friction angle and cohesion increase with the volume percentage of LSCs, but these quantities do not increase linearly with the percentage of LSCs. Young's modulus does not show increase with the LSC amount.

(3) The choice of values for the interfacial cohesion between LSC and matrix is important when determining the strength because these interfaces can serve as sites for crack initiation if the cohesion value is the lowest among the possible types of interfaces in the sample. Care must be exercised when choosing this value.

References

Cundall, P.A. (2000), Numerical experiments on rough joints in shear using a bonded particle model, *In: Aspects of tectonic faulting (edited by Lehner, F.K. & Urai, J.L.)*, Springer-Verlag, Berlin, 1-9

Hobbs, B.E., Ord, A., Regenauer-Lieb, K., Boschetti, F., Zhang, Y. & Durrlemann, S. (2004), Ab initio emergent phenomena in PFC, *In: Numerical modeling in micromechanics via particle methods - 2004 (edited by Shimizu, Y., Hart, R. & Cundall, P.)*, A.A. Balkema Publishers, Leiden, 235-239

Itasca Consultant Group (1995), PFC 2D manual, Version 1.1., Minneapolis

Lee, C., Park, Y. & Kwon, S. (2004), Simulation of two-dimensional 'thin-skinned' orogenic wedge using PFC, *In: Numerical modeling in micromechanics via particle methods - 2004 (edited by Shimizu, Y., Hart, R. & Cundall, P.)*, A.A. Balkema Publishers, Leiden, 181-186

Park, E.S., Marin, C.D. & Christiansson, R. (2004), Numerical simulation of the discontinuous behavior of rock masses, *In: Numerical modeling in micromechanics via particle methods - 2004 (edited by Shimizu, Y., Hart, R. & Cundall, P.)*, A.A. Balkema Publishers, Leiden, 85-91

Park, Y., Lee, C. & Ree, J.-H. (2004), Simulation of magmatic fabrics using PFC, *In: Numerical modeling in micromechanics via particle methods - 2004 (edited by Shimizu, Y., Hart, R. & Cundall, P.)*, A.A. Balkema Publishers, Leiden, 175-179

Potyondy, D.O., Cundall, P.A. & Lee, C. (1996), Modeling rock using bonded assemblies of circular particles, *In: Rock mechanics tool and techniques (edited by Aubertin, M., Hassani, F. & Mitri, H.)*, A.A. Balkema Publishers, Rotterdam, 1937-1944

Shimizu, Y., Hart, R. & Cundall, P. (eds). (2004), Numerical modeling in micromechanics via particle methods - 2004, A.A. Balkema Publishers, Leiden, 435 p.